Available online at www.sciencedirect.com
SCIENCE DIRECT®
International Journal of Solids and Structures 42 (2005) 239–253
INTERNATIONAL JOURNAL OF SOLIDS and STRUCTURES
www.elsevier.com/locate/ijsolstr

Buckling of short beams with warping effect included

Hsiang-Chuan Tsai [a,*], James M. Kelly [b]

[a] Department of Construction Engineering, National Taiwan University of Science and Technology, P.O. Box 90-130, Taipei 106, Taiwan
[b] Pacific Earthquake Engineering Research Center, University of California, Berkeley, CA 94804, USA

Received 22 September 2003; received in revised form 20 July 2004
Available online 18 September 2004

Abstract

A beam theory for the stability analysis of short beam that includes shear deformation and warping of the cross-section is developed. The warping of the cross-section is taken to be an independent kinematics quantity and corresponding force resultants are defined. For the beam subjected to the external loading only at the ends of the beam, equilibrium equations have been obtained by the principle of virtual work. The variations of lateral displacement, rotational angle of the cross-section and the multiplier of the warping shape along the beam axis are solved in closed form and expressed in terms of deformation quantities at the ends of the beam. Based on this beam theory, the lateral stiffness of the beam sustained an axial compression force and a lateral shear force at one end is explicitly derived, from which the equation of the buckling load is established and the buckling load can be solved. When the effect of cross-section warping is neglected, the derived lateral stiffness and buckling load converge to the solutions of the Haringx theory.

Keywords: Beam theory; Buckling; Warping

1. Introduction

A multilayer elastomeric bearing used for the seismic or vibration isolation of buildings or equipments is susceptible to a type of buckling instability similar to that of an ordinary column, even though it is a relatively squat component. As the shear stiffness of an isolator can be two orders of magnitude smaller than the compression stiffness or the resistance to bending, the deformation of this type of isolator is dominated

* Corresponding author. Tel.: +886 227 376581; fax: +886 227 376606.
E-mail address: hctsai@mail.ntust.edu.tw (H.-C. Tsai).

0020-7683/$ - see front matter
doi:10.1016/j.ijsolstr.2004.07.021

by shear. The large stiffness difference is achieved by having many layers of elastomer (usually comprised of natural rubber) reinforced by steel plates. The reinforcing plates constrain the elastomer from lateral expansion and provide a high vertical and bending stiffness, but have no effect on the shear stiffness.

Since the isolators are always used to carry vertical load, it is essential that their stability can be assessed in a reasonably simple manner. For this reason, a buckling analysis is used that treats the isolator as a composite column with low shear stiffness. In the standard approach, the bearing is assumed to be a beam, and plane sections, normal to the undeformed axis before deformation, are assumed to remain plane but not necessarily normal after deformation. The theory is an outgrowth of work by Haringx on the mechanical characteristics of helical steel springs and rubber rods used for vibration mounting. This work was published as a series of technical reports, the third of which (Haringx, 1948) covers the stability of rubber rods. The Haringx theory was later applied by Gent (1964) to multilayer elastomeric bearings. Tsai and Hsueh (2001) extended the Haringx theory to the viscoelastic column to study the behavior of isolation bearings that possess an energy-dissipation capacity.

The assumption that plane sections remain plane disables the Haringx theory from studying the influence of the flexibility of the reinforcing plates on the buckling of the isolator. In this paper, a theory is developed that extends the Haringx theory by allowing the cross-sections to deform into a non-planar surface. The warping of the cross-section, which is permitted by the flexibility of the reinforcing sheets, is taken into account by introducing a kinematics displacement function that produces no rotation of the section but measures the deviation from plane of the deformed cross-section. Force resultants that arise from the presence of this kinematics quantity are also introduced and constitutive equations for these quantities are derived. The appropriate equations of equilibrium incorporating these new force quantities are developed. The lateral stiffness and buckling load that include the shear and warping effects are derived for the beam subjected to an axial compression force and a lateral shear force at one end of the beam. It should be noted that the terminology of warping used here is not associated with torsion; it just specifies the distortion of the cross-section created by moment and shear.

2. Governing equations

The prismatic beam shown in Fig. 1 adopts a rectangular coordinate system such that the X and Y-axes lie in the cross-section and the Z-axis coincides with the axis of centroids along the beam. The cross-section is symmetric to the X and Y-axes. Flexural deformation is assumed to take place in the X–Z plane. The displacements of the beam in the X and Z directions, denoted as $\bar{u}$ and $\overline{w}$ respectively, are taken to be

$$\bar{u}(X,Z) = \upsilon(Z) \tag{1}$$

$$\overline{w}(X,Z) = -\Delta(Z) - X\psi(Z) + \Omega(X)\phi(Z) \tag{2}$$

which indicates that the deformation of the beam is characterized by the four displacement functions of Z coordinate: υ as the lateral displacement at the centroid of the cross-section in the X direction, Δ as the axial displacement at the centroid of the cross-section in the negative Z direction, ψ as the average angle of rotation of the cross-section in the Y direction, and ϕ as the multiplier of the warping function Ω which is a prescribed function of X defining the warping shape of the cross-section. The rotation of the cross-section ψ is assumed as a small angle. The deviation of the cross-section of the deformed beam from a plane surface is measured by $\Omega(X)\phi(Z)$. The selection of Ω to be dimensionless means the warping multiplier ϕ has units of displacement. According to infinitesimal strain definitions, the resulting normal strain ε_{ZZ} and shear strain γ_{XZ} are

$$\varepsilon_{ZZ} = \overline{w}_{,Z} = -\Delta_{,Z} - X\psi_{,Z} + \Omega\phi_{,Z} \tag{3}$$

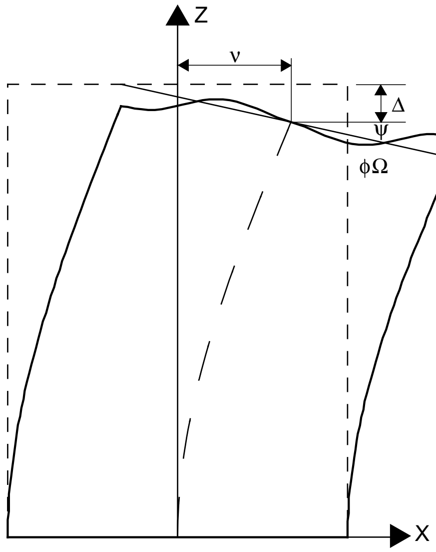

Fig. 1. Deformation of beam with cross-section warping.

$$\gamma_{XZ} = \bar{u}_{,Z} + \overline{w}_{,X} = \upsilon_{,Z} - \psi + \Omega_{,X}\phi \tag{4}$$

where the commas imply partial differentiation with respect to the indicated coordinate.

Large lateral deformation can change the length of the beam. To calculate this effect, the lateral deformation of an infinitesimal section of the beam is depicted in Fig. 2. For clarity, the warping of cross-section is not plotted in the figure. At first, the section has a rigid rotation $\theta_1 = \overline{w}_{,X}$ that creates a vertical movement

$$\Delta_1 = \mathrm{d}Z - \mathrm{d}Z\cos\theta_1 \approx \frac{1}{2}\theta_1^2\mathrm{d}Z \tag{5}$$

Then, the shear deformation is applied to the rotated section and forms the angle $\theta_2 = \gamma_{XZ}$ that makes a vertical movement

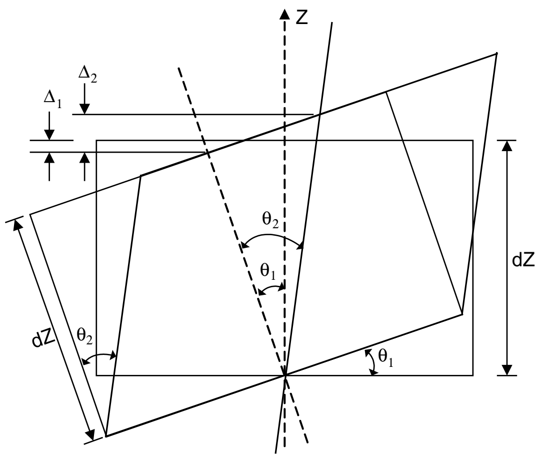

Fig. 2. Vertical displacement created by large lateral deformation.

$$\Delta_2 = (\mathrm{d}Z \tan\theta_2)\sin\theta_1 \approx \theta_1\theta_2 \mathrm{d}Z \tag{6}$$

Therefore, the total vertical movement created by the lateral deformation is

$$\Delta_2 - \Delta_1 = \left(\gamma_{XZ}\overline{w}_{,X} - \frac{1}{2}\overline{w}_{,X}^2\right)\mathrm{d}Z \tag{7}$$

Using Eq. (4), the corresponding axial strain becomes

$$\varepsilon = \frac{\Delta_2 - \Delta_1}{\mathrm{d}Z} = \frac{1}{2}(\psi - \Omega_{,X}\phi)^2 - \upsilon_{,Z}(\psi - \Omega_{,X}\phi) \tag{8}$$

Including this deformation effect, the internal virtual work of the beam has the following variation form

$$\delta W_i = \int_0^h \int_A [\sigma_{ZZ}\delta(\varepsilon_{ZZ} - \varepsilon) + \tau_{XZ}\delta\gamma_{XZ}]\mathrm{d}A\,\mathrm{d}Z \tag{9}$$

in which the integration is carried out over the undeformed shape, h is the length of the undeformed beam and A is the area of the undeformed cross-section. The normal stress σ_{ZZ} and shear stress τ_{XZ} are based on infinitesimal deformation. Different from the consistent approach of buckling analysis that requires the use of finite deformation theory, we use the infinitesimal deformation theory to define the strain and stress. The nonlinear effect caused by the buckling is then introduced through Eq. (8). Because the main issues here are the buckling load and the stiffness reduction before buckling, not the post-buckling behavior, the error arisen from this simplified approach is negligible. From Eq. (9), if the shear deformation and cross-section warping are neglected, the same governing equations for beam buckling can be established as those derived from force equilibrium in the textbook of strength of materials.

Using Eq. (3), the virtual work done by the normal stress becomes

$$\int_0^h \int_A \sigma_{ZZ}\delta\varepsilon_{ZZ}\,\mathrm{d}A\,\mathrm{d}Z = \int_0^h (N\delta\Delta_{,Z} + M\delta\psi_{,Z} + Q\delta\phi_{,Z})\mathrm{d}Z \tag{10}$$

in which N is the axial compression force,

$$N = -\int_A \sigma_{ZZ}\,\mathrm{d}A \tag{11}$$

M is the bending moment,

$$M = -\int_A \sigma_{ZZ}X\,\mathrm{d}A \tag{12}$$

and Q is called the warping moment,

$$Q = \int_A \sigma_{ZZ}\Omega\,\mathrm{d}A \tag{13}$$

which has units of force.

Using Eq. (4), the virtual work done by the shear stress becomes

$$\int_0^h \int_A \tau_{XZ}\delta\gamma_{XZ}\,\mathrm{d}A\,\mathrm{d}Z = \int_0^h [V\delta(\upsilon_{,Z} - \psi) + R\delta\phi]\mathrm{d}Z \tag{14}$$

in which V is the shear force,

$$V = \int_A \tau_{XZ}\,\mathrm{d}A \tag{15}$$

and R is called the warping shear,

$$R = \int_A \tau_{XZ} \Omega_{,X} \, \mathrm{d}A \tag{16}$$

which has units of force per length.

Taking integration by part, the internal virtual work in Eq. (9) becomes

$$\begin{aligned} \delta W_i = {} & N\delta\Delta|_0^h + M\delta\psi|_0^h + Q\delta\phi|_0^h + (V - N\psi + N_B\phi)\delta\upsilon|_0^h - \int_0^h N_{,Z}\,\delta\Delta\,\mathrm{d}Z \\ & - \int_0^h [M_{,Z} + V + N(\upsilon_{,Z} - \psi) + N_B\phi]\delta\psi\,\mathrm{d}Z - \int_0^h [Q_{,Z} - R - N_B(\upsilon_{,Z} - \psi) - N_C\phi]\delta\phi\,\mathrm{d}Z \\ & - \int_0^h (V - N\psi + N_B\phi)_{,Z}\,\delta\upsilon\,\mathrm{d}Z \end{aligned} \tag{17}$$

in which N_B and N_C are two normal forces related to cross-section warping, defined as

$$N_B = -\int_A \sigma_{ZZ}\Omega_{,X}\,\mathrm{d}A \tag{18}$$

$$N_C = -\int_A \sigma_{ZZ}\Omega_{,X}^2\,\mathrm{d}A \tag{19}$$

If the external forces act at the ends of the beam only, the principle of virtual work generates the following equilibrium equations

$$N_{,Z} = 0 \tag{20}$$

$$(V - N\psi + N_B\phi)_{,Z} = 0 \tag{21}$$

$$M_{,Z} + V + N(\upsilon_{,Z} - \psi) + N_B\phi = 0 \tag{22}$$

$$Q_{,Z} - R - N_B(\upsilon_{,Z} - \psi) - N_C\phi = 0 \tag{23}$$

These are the same as the equations solved directly from force equilibrium (Kelly, 1994).

For the homogeneous elastic beam, the shear stress has the form, from Eq. (4),

$$\tau_{XZ} = G(\upsilon_{,Z} - \psi + \Omega_{,X}\phi) \tag{24}$$

with G being the shear modulus. Substituting this into Eqs. (15) and (16), respectively, gives

$$V = GA(\upsilon_{,Z} - \psi) + GB\phi \tag{25}$$

$$R = GB(\upsilon_{,Z} - \psi) + GC\phi \tag{26}$$

in which B and C are cross-section properties of warping defined as

$$B = \int_A \Omega_{,X}\,\mathrm{d}A \quad \text{and} \quad C = \int_A \Omega_{,X}^2\,\mathrm{d}A \tag{27}$$

From Eqs. (25) and (26), Eq. (24) becomes

$$\tau_{XZ} = \left(\frac{C - B\Omega_{,X}}{AC - B^2}\right)V - \left(\frac{B - A\Omega_{,X}}{AC - B^2}\right)R \tag{28}$$

For the homogeneous elastic beam, the normal stress has the form, from Eq. (3),

$$\sigma_{ZZ} = E(-\Delta_{,Z} - X\psi_{,Z} + \Omega\phi_{,Z}) \tag{29}$$

with E being the elastic modulus. It is convenient to select the warping function Ω such that the axial force N defined in Eq. (11) and the bending moment M defined in Eq. (12) are independent of Ω. The appropriate form of the warping function Ω must satisfy the following condition

$$\int_A \Omega \, \mathrm{d}A = 0 \tag{30}$$

$$\int_A X\Omega \, \mathrm{d}A = 0 \tag{31}$$

For the cross-section that is symmetric to the X and Y-axes, Eq. (30) indicates that the warping function Ω is an odd function of X. There are many forms that the warping function could take, but Eq. (31) implies that the simplest warping function is a cubic polynomial with a form

$$\Omega(X) = \left(\frac{X}{a}\right)^3 + \omega\left(\frac{X}{a}\right) \tag{32}$$

in which a is a dimension of the cross-section in the X direction and ω is a constant determined from Eq. (31).

Substituting Eq. (29) into Eq. (11) gives

$$N = EA\Delta_{,Z} \tag{33}$$

Substituting Eq. (29) into Eqs. (12) and (13), respectively, and using the property in Eq. (31) give

$$M = EI\psi_{,Z} \tag{34}$$

$$Q = EJ\phi_{,Z} \tag{35}$$

in which I is the second moment of area defined as

$$I = \int_A X^2 \, \mathrm{d}A \tag{36}$$

and J is a cross-section property of the warping shape defined as

$$J = \int_A \Omega^2 \, \mathrm{d}A \tag{37}$$

Therefore, Eq. (29) becomes

$$\sigma_{ZZ} = -\frac{N}{A} - X\frac{M}{I} + \Omega\frac{Q}{J} \tag{38}$$

Because $\Omega_{,X}$ is an even function of X, substituting Eq. (38) into Eqs. (18) and (19) lead to

$$N_B = \frac{B}{A}N \tag{39}$$

$$N_C = \frac{C}{A}N \tag{40}$$

Eq. (38) indicates that the stress created by the axial force is uniform in the cross-section and the stress created by the bending moment is linearly varied for the homogeneous beams. For the reinforced isolators, the stress distribution is different from Eq. (38), so that the expressions of axial stiffness EA, bending stiffness EI and warping stiffness EJ are different from the expressions in the homogeneous beam.

3. General solution

When the external loading acts only at the ends of the beam, the vertical and horizontal force resultants acting on the cross-section are constant through the beam. From Eqs. (20) and (21), we have

$$N = P \tag{41}$$

$$V - N\psi + N_B\phi = F \tag{42}$$

where P is the vertical compression force acting on the beam and F is the horizontal shear force acting on the beam.

Substituting Eq. (25) into Eq. (42) gives

$$\upsilon_{,Z} = \left(1 + \frac{P}{GA}\right)\psi - \left(\frac{GB + N_B}{GA}\right)\phi + \frac{F}{GA} \tag{43}$$

Substituting Eqs. (25) and (34) into Eq. (22) and using Eq. (43) to eliminate the term of $\upsilon_{,Z}$ lead to

$$\phi = \frac{GA}{GB + N_B}\left[\frac{EI}{P}\psi_{,ZZ} + \left(1 + \frac{P}{GA}\right)\psi + \left(1 + \frac{P}{GA}\right)\frac{F}{P}\right] \tag{44}$$

Substituting Eqs. (26) and (35) into Eq. (23) and using Eq. (43) to eliminate the term of $\upsilon_{,Z}$ lead to

$$\psi = \frac{GA}{(GB + N_B)P}\left\{EJ\phi_{,ZZ} + \left[\frac{(GB + N_B)^2}{GA} - (GC + N_C)\right]\phi\right\} - \frac{F}{P} \tag{45}$$

Substituting Eq. (44) into Eq. (45) yields

$$\psi_{,ZZZZ} + \frac{\overline{P}(1 + \overline{P}) + \kappa_b - \kappa_c}{\rho h^2}\psi_{,ZZ} - \frac{\overline{P}[(1 + \overline{P})\kappa_c - \kappa_b]}{\rho^2 h^4}\psi = \frac{\overline{P}[(1 + \overline{P})\kappa_c - \kappa_b]}{\rho^2 h^4}\frac{F}{P} \tag{46}$$

in which $\overline{P}$ is the dimensionless compression force defined as

$$\overline{P} = \frac{P}{GA} \tag{47}$$

ρ is the ratio of the flexure rigidity to shear rigidity

$$\rho = \frac{EI}{GAh^2} \tag{48}$$

κ_b and κ_c are two parameters corresponding to cross-section warping

$$\kappa_b = \frac{EI}{EJ}\left(\frac{GB + N_B}{GA}\right)^2 \tag{49}$$

$$\kappa_c = \frac{EI}{EJ}\left(\frac{GC + N_C}{GA}\right) \tag{50}$$

If the complementary solution of ψ in Eq. (46) has the form $\psi = e^{mZ}$, then m can be solved from

$$m^4 + \frac{\overline{P}(1 + \overline{P}) + \kappa_b - \kappa_c}{\rho h^2}m^2 - \frac{\overline{P}[(1 + \overline{P})\kappa_c - \kappa_b]}{\rho^2 h^4} = 0 \tag{51}$$

which gives

$$m^2 = -\frac{\beta_1}{2\rho h^2} \quad \text{and} \quad m^2 = \frac{\beta_2}{2\rho h^2} \tag{52}$$

with

$$\beta_1 = [\overline{P}(1+\overline{P}) + \kappa_b - \kappa_c] + \sqrt{[\overline{P}(1+\overline{P}) + \kappa_b - \kappa_c]^2 + 4\overline{P}[(1+\overline{P})\kappa_c - \kappa_b]} \tag{53}$$

$$\beta_2 = -[\overline{P}(1+\overline{P}) + \kappa_b - \kappa_c] + \sqrt{[\overline{P}(1+\overline{P}) + \kappa_b - \kappa_c]^2 + 4\overline{P}[(1+\overline{P})\kappa_c - \kappa_b]} \tag{54}$$

The parameters β_1 and β_2 are real number, because the term inside the square root in Eqs. (53) and (54), which equals to $[\overline{P}(1+\overline{P}) - (\kappa_b - \kappa_c)]^2 + 4\kappa_b\overline{P}^2$, is always positive. For $(1+\overline{P})\kappa_c - \kappa_b \geqslant 0$, it knows $\beta_1 \geqslant 0$ and $\beta_2 \geqslant 0$. For $(1+\overline{P})\kappa_c - \kappa_b < 0$, it knows $\beta_1 \geqslant 0$ but $\beta_2 < 0$. The solutions of m are

$$m = \pm \mathrm{i}\sqrt{\frac{\beta_1}{2\rho h^2}} \quad \text{and} \quad m = \pm\sqrt{\frac{\beta_2}{2\rho h^2}} \tag{55}$$

in which $\mathrm{i} = \sqrt{-1}$.

The general solution of ψ to Eq. (46) has the form

$$\psi = c_1 \cos\sqrt{\frac{\beta_1}{2\rho}}\frac{Z}{h} + c_2 \sin\sqrt{\frac{\beta_1}{2\rho}}\frac{Z}{h} + c_3 \cosh\sqrt{\frac{\beta_2}{2\rho}}\frac{Z}{h} + c_4 \sinh\sqrt{\frac{\beta_2}{2\rho}}\frac{Z}{h} - \frac{F}{P} \tag{56}$$

in which c_i is the constant determined from boundary conditions. Substituting the above equation into Eq. (44) gives

$$\phi = \frac{GA}{GB + N_B}\left[\left(1 + \overline{P} - \frac{\beta_1}{2\overline{P}}\right)\left(c_1 \cos\sqrt{\frac{\beta_1}{2\rho}}\frac{Z}{h} + c_2 \sin\sqrt{\frac{\beta_1}{2\rho}}\frac{Z}{h}\right) + \left(1 + \overline{P} + \frac{\beta_2}{2\overline{P}}\right)\right.$$
$$\left.\times\left(c_3 \cosh\sqrt{\frac{\beta_2}{2\rho}}\frac{Z}{h} + c_4 \sinh\sqrt{\frac{\beta_2}{2\rho}}\frac{Z}{h}\right)\right] \tag{57}$$

Substituting Eqs. (56) and (57) into Eq. (43) gives

$$v_{,Z} = \frac{\beta_1}{2\overline{P}}\left(c_1 \cos\sqrt{\frac{\beta_1}{2\rho}}\frac{Z}{h} + c_2 \sin\sqrt{\frac{\beta_1}{2\rho}}\frac{Z}{h}\right) - \frac{\beta_2}{2\overline{P}}\left(c_3 \cosh\sqrt{\frac{\beta_2}{2\rho}}\frac{Z}{h} + c_4 \sinh\sqrt{\frac{\beta_2}{2\rho}}\frac{Z}{h}\right) - \frac{F}{P} \tag{58}$$

from which

$$v = \frac{h}{\overline{P}}\sqrt{\frac{\rho\beta_1}{2}}\left[c_1 \sin\sqrt{\frac{\beta_1}{2\rho}}\frac{Z}{h} + c_2\left(1 - \cos\sqrt{\frac{\beta_1}{2\rho}}\frac{Z}{h}\right)\right]$$
$$-\frac{h}{\overline{P}}\sqrt{\frac{\rho\beta_2}{2}}\left[c_3 \sinh\sqrt{\frac{\beta_2}{2\rho}}\frac{Z}{h} + c_4\left(\cosh\sqrt{\frac{\beta_2}{2\rho}}\frac{Z}{h} - 1\right)\right] - \frac{F}{P}Z + v(0) \tag{59}$$

By assigning $Z = 0$ and $Z = h$ into Eqs. (56),(57) and (59), we can solve the constants as

$$c_1 = \frac{2\overline{P}}{\beta_1 + \beta_2}\left\{\left(1 + \overline{P} + \frac{\beta_2}{2\overline{P}}\right)\left[\frac{F}{P} + \psi(0)\right] - \frac{GB + N_B}{GA}\phi(0)\right\} \tag{60}$$

$$c_2 = \frac{2\overline{P}}{(\beta_1+\beta_2)\sin\sqrt{\frac{\beta_1}{2\rho}}}\left\{\left(1+\overline{P}+\frac{\beta_2}{2\overline{P}}\right)\left[\frac{F}{P}\left(1-\cos\sqrt{\frac{\beta_1}{2\rho}}\right)+\psi(h)-\psi(0)\cos\sqrt{\frac{\beta_1}{2\rho}}\right]\right.$$
$$\left.-\frac{GB+N_B}{GA}\left[\phi(h)-\phi(0)\cos\sqrt{\frac{\beta_1}{2\rho}}\right]\right\} \tag{61}$$

$$c_3 = \frac{2\overline{P}}{\beta_1+\beta_2}\left\{-\left(1+\overline{P}-\frac{\beta_1}{2\overline{P}}\right)\left[\frac{F}{P}+\psi(0)\right]+\frac{GB+N_B}{GA}\phi(0)\right\} \tag{62}$$

$$c_4 = \frac{2\overline{P}}{(\beta_1+\beta_2)\sinh\sqrt{\frac{\beta_2}{2\rho}}}\left\{-\left(1+\overline{P}-\frac{\beta_1}{2\overline{P}}\right)\left[\frac{F}{P}\left(1-\cosh\sqrt{\frac{\beta_2}{2\rho}}\right)+\psi(h)-\psi(0)\cosh\sqrt{\frac{\beta_2}{2\rho}}\right]\right.$$
$$\left.+\frac{GB+N_B}{GA}\left[\phi(h)-\phi(0)\cosh\sqrt{\frac{\beta_2}{2\rho}}\right]\right\} \tag{63}$$

with

$$\frac{F}{P} = \left\{\frac{(\beta_1+\beta_2)}{\sqrt{2\rho}}\left[\frac{\upsilon(h)-\upsilon(0)}{h}\right]-\left[\left(1+\overline{P}+\frac{\beta_2}{2\overline{P}}\right)\sqrt{\beta_1}\tan\sqrt{\frac{\beta_1}{8\rho}}+\left(1+\overline{P}-\frac{\beta_1}{2\overline{P}}\right)\sqrt{\beta_2}\tanh\sqrt{\frac{\beta_2}{8\rho}}\right][\psi(h)\right.$$
$$\left.+\psi(0)]+\left(\sqrt{\beta_1}\tan\sqrt{\frac{\beta_1}{8\rho}}+\sqrt{\beta_2}\tanh\sqrt{\frac{\beta_2}{8\rho}}\right)\left(\frac{GB+N_B}{GA}\right)[\phi(h)+\phi(0)]\right\}$$
$$\Bigg/\left\{2\left[\left(1+\overline{P}+\frac{\beta_2}{2\overline{P}}\right)\sqrt{\beta_1}\tan\sqrt{\frac{\beta_1}{8\rho}}+\left(1+\overline{P}-\frac{\beta_1}{2\overline{P}}\right)\sqrt{\beta_2}\tanh\sqrt{\frac{\beta_2}{8\rho}}\right]-\frac{(\beta_1+\beta_2)}{\sqrt{2\rho}}\right\} \tag{64}$$

4. Lateral stiffness and buckling load

For the beam shown in Fig. 3, its lower end is fixed against any displacement, rotation and warping, whereas the upper end is allowed to move horizontally and vertically but is still constrained against rotation

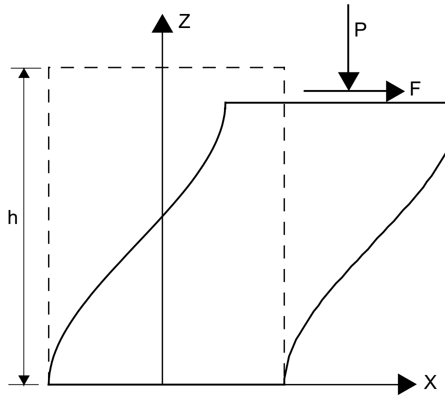

Fig. 3. Beam subjected to axial compression and lateral shear at one end.

and warping. The upper end of the beam is subjected to a compressive force P and a horizontal force F. The lateral stiffness of the beam is defined as

$$K_{\mathrm{H}} = \frac{F}{\upsilon(h)} \tag{65}$$

Substituting the boundary conditions at the lower end, $\upsilon(0) = 0$, $\psi(0) = 0$ and $\phi(0) = 0$, and at the upper end, $\psi(h) = 0$ and $\phi(h) = 0$, into Eq. (64), the lateral stiffness of the beam can be solved as

$$K_{\mathrm{H}} = \left(\frac{GA}{h}\right)\frac{\overline{P}}{\frac{2\overline{P}(1+\overline{P})+\beta_2}{\overline{P}(\beta_1+\beta_2)}\sqrt{2\rho\beta_1}\tan\sqrt{\frac{\beta_1}{8\rho}} + \frac{2\overline{P}(1+\overline{P})-\beta_1}{\overline{P}(\beta_1+\beta_2)}\sqrt{2\rho\beta_2}\tanh\sqrt{\frac{\beta_2}{8\rho}} - 1} \tag{66}$$

which is the solution for $(1+\overline{P})\kappa_c - \kappa_b \geqslant 0$. When $(1+\overline{P})\kappa_c - \kappa_b < 0$, then $\beta_2 < 0$, the above equation can be expressed in terms of real numbers as

$$K_{\mathrm{H}} = \left(\frac{GA}{h}\right)\frac{\overline{P}}{\frac{2\overline{P}(1+\overline{P})+\beta_2}{\overline{P}(\beta_1+\beta_2)}\sqrt{2\rho\beta_1}\tan\sqrt{\frac{\beta_1}{8\rho}} - \frac{2\overline{P}(1+\overline{P})-\beta_1}{\overline{P}(\beta_1+\beta_2)}\sqrt{2\rho|\beta_2|}\tan\sqrt{\frac{|\beta_2|}{8\rho}} - 1} \tag{67}$$

When the lateral stiffness equals zero, the beam becomes unstable and the corresponding compression force is referred to as buckling load P_{cr}. In Eq. (66), $K_{\mathrm{H}} = 0$ when

$$\sqrt{\frac{\beta_1}{8\rho}} = \frac{\pi}{2} \tag{68}$$

In Eq. (67), $K_{\mathrm{H}} = 0$ when

$$\sqrt{\frac{\beta_1}{8\rho}} = \frac{\pi}{2} \quad \text{or} \quad \sqrt{\frac{|\beta_2|}{8\rho}} = \frac{\pi}{2} \tag{69}$$

Using Eqs. (53) and (54), the conditions in Eqs. (68) and (69) give the same equation

$$\overline{P}[(1+\overline{P})\kappa_c - \kappa_b] + \pi^2\rho[\overline{P}(1+\overline{P}) + \kappa_b - \kappa_c] - \pi^4\rho^2 = 0 \tag{70}$$

which is the equation being applied to solve the buckling load of the beam.

To find lateral stiffness without compressive load, assume $\overline{P} \ll 1$ and apply the following series expansion

$$\sqrt{1+x} \approx 1 + \frac{1}{2}x - \frac{1}{8}x^2 + \cdots \tag{71}$$

on Eqs. (53) and (54). When $(1+\overline{P})\kappa_c - \kappa_b > 0$, this gives

$$\beta_1 \approx 2\overline{P}\left(1 + \frac{\kappa_c}{\kappa_c - \kappa_b}\overline{P}\right) \quad \text{and} \quad \beta_2 \approx 2(\kappa_c - \kappa_b) \tag{72}$$

Substituting these into Eq. (66) and neglecting high-order terms of $\overline{P}$ lead to

$$K_{\mathrm{H}} = \left(\frac{GA}{h}\right)\frac{1}{1 + \frac{1}{12\rho} + \frac{\kappa_b}{\kappa_c-\kappa_b}\left[1 - \left(\tanh\sqrt{\frac{\kappa_c-\kappa_b}{4\rho}}\right)\Big/\sqrt{\frac{\kappa_c-\kappa_b}{4\rho}}\right]} \tag{73}$$

When $(1+\overline{P})\kappa_c - \kappa_b < 0$,

$$\beta_1 \approx 2(\kappa_b - \kappa_c) \quad \text{and} \quad \beta_2 \approx -2\overline{P}\left(1 + \frac{\kappa_c}{\kappa_c - \kappa_b}\overline{P}\right) \tag{74}$$

Substituting these into Eq. (67) and neglecting high-order terms of $\overline{P}$ give

$$K_{\mathrm{H}} = \left(\frac{GA}{h}\right)\frac{1}{1+\frac{1}{12\rho}-\frac{\kappa_b}{\kappa_b-\kappa_c}\left[1-\left(\tan\sqrt{\frac{\kappa_b-\kappa_c}{4\rho}}\right)\Big/\sqrt{\frac{\kappa_b-\kappa_c}{4\rho}}\right]} \tag{75}$$

Eq. (73) is the solution of K_{H} at $P=0$ when $\kappa_c > \kappa_b$. Eq. (75) is the solution of K_{H} at $P=0$ when $\kappa_c < \kappa_b$.

If the effect of cross-section warping is not considered, we can set $EJ \to \infty$, such that $\kappa_b = 0$ and $\kappa_c = 0$ which give, from Eqs. (53) and (54),

$$\beta_1 = 2\overline{P}(1+\overline{P}) \quad \text{and} \quad \beta_2 = 0 \tag{76}$$

Substituting these into Eq. (66) gives

$$K_{\mathrm{H}} = \left(\frac{GA}{h}\right)\frac{\overline{P}}{\sqrt{\frac{4\rho(1+\overline{P})}{\overline{P}}}\tan\sqrt{\frac{\overline{P}(1+\overline{P})}{4\rho}}-1} \tag{77}$$

When $\overline{P} \to 0$, the above equation becomes

$$K_{\mathrm{H}} = \left(\frac{GA}{h}\right)\frac{1}{1+\frac{12}{\rho}} \tag{78}$$

which means, from Eq. (48),

$$\frac{1}{K_{\mathrm{H}}} = \frac{h}{GA} + \frac{h^3}{12EI} \tag{79}$$

In Eq. (77), $K_{\mathrm{H}} = 0$ when

$$\sqrt{\frac{\overline{P}(1+\overline{P})}{4\rho}} = \frac{\pi}{2} \tag{80}$$

from which the buckling load of the beam without cross-section warping can be solved as

$$P_{\mathrm{cr}} = GA\left(\frac{-1+\sqrt{1+4\pi^2\rho}}{2}\right) \tag{81}$$

which is the same as the solution derived by Haringx's theory (Kelly, 1997).

5. Examples of homogeneous beams

If the beam is homogeneous and has symmetric cross-section, substituting Eqs. (39) and (40) into Eqs. (49) and (50), respectively, leads to

$$\kappa_b = \frac{1}{J}\left(\frac{B}{A}\right)^2(1+\overline{P})^2 \tag{82}$$

$$\kappa_c = \frac{1}{J}\left(\frac{C}{A}\right)(1+\overline{P}) \tag{83}$$

For the rectangular cross-section having a side length $2a$ along the X-axis and $2b$ along the Y-axis, the warping function that satisfies the condition in Eq. (31) is

$$\Omega(X) = \left(\frac{X}{a}\right)^3 - \frac{3}{5}\left(\frac{X}{a}\right) \tag{84}$$

Substituting this into Eqs. (37) and (27) gives $J = \frac{16}{175}ba$, $B = \frac{8}{5}b$ and $C = \frac{96}{25}\frac{b}{a}$. The other cross-sectional properties are $A = 4ba$ and $I = \frac{4}{3}ba^3$. The warping parameters in Eqs. (82) and (83) become

$$\kappa_b = \frac{7}{3}(1+\overline{P})^2 \quad \text{and} \quad \kappa_c = 14(1+\overline{P}) \tag{85}$$

which satisfy the condition $(1+\overline{P})\kappa_c - \kappa_b \geqslant 0$. The parameters β_1 and β_2 in Eqs. (53) and (54) become

$$\beta_1 = \frac{10}{3}(1+\overline{P})\left[\left(\overline{P}-\frac{7}{2}\right) + \sqrt{\left(\overline{P}-\frac{7}{2}\right)^2 + \frac{21}{5}\overline{P}}\right] \tag{86}$$

$$\beta_2 = \frac{10}{3}(1+\overline{P})\left[-\left(\overline{P}-\frac{7}{2}\right) + \sqrt{\left(\overline{P}-\frac{7}{2}\right)^2 + \frac{21}{5}\overline{P}}\right] \tag{87}$$

Substituting these parameters into Eq. (66), the dimensionless lateral stiffness $K_{\mathrm{H}}h/(GA)$ becomes a function of ρ and $\overline{P}$. The variations of the lateral stiffness with the compression force for different ρ values are plotted in Fig. 4, which reveals that the lateral stiffness decreases with increasing compression force or reducing ρ value. The lateral stiffness at $P = 0$ is calculated from Eq. (73).

For the circular cross-section of radius a, the warping function is

$$\Omega(X) = \left(\frac{X}{a}\right)^3 - \frac{1}{2}\left(\frac{X}{a}\right) \tag{88}$$

Substituting this into Eqs. (37) and (27) gives $J = \frac{\pi}{64}a^2$, $B = \frac{\pi}{4}a$ and $C = \frac{5\pi}{8}$. The other cross-sectional properties are $A = \pi a^2$ and $I = \frac{\pi}{4}a^4$. The warping parameters in Eqs. (82) and (83) become

$$\kappa_b = (1+\overline{P})^2 \quad \text{and} \quad \kappa_c = 10(1+\overline{P}) \tag{89}$$

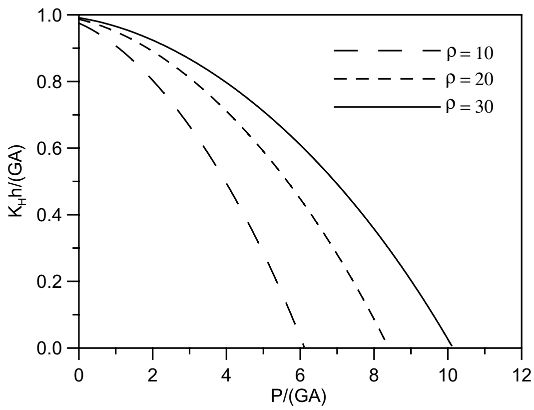

Fig. 4. Lateral stiffness of rectangular beams varied with compression load.

which satisfy the condition $(1+\overline{P})\kappa_c - \kappa_b \geqslant 0$. The parameters β_1 and β_2 in Eqs. (53) and (54) become

$$\beta_1 = 2(1+\overline{P})\left[\left(\overline{P}-\frac{9}{2}\right)+\sqrt{\left(\overline{P}-\frac{9}{2}\right)^2+9\overline{P}}\right] \tag{90}$$

$$\beta_2 = 2(1+\overline{P})\left[-\left(\overline{P}-\frac{9}{2}\right)+\sqrt{\left(\overline{P}-\frac{9}{2}\right)^2+9\overline{P}}\right] \tag{91}$$

Substituting these parameters into Eq. (66), the dimensionless lateral stiffness $K_\mathrm{H}h/(GA)$ becomes a function of ρ and $\overline{P}$. Similar to the rectangular section, the variations of the lateral stiffness with the compression force for several ρ values plotted in Fig. 5 reveal that the lateral stiffness decreases with increasing compression force or reducing ρ value. The lateral stiffness at $P = 0$ is calculated from Eq. (73).

The lateral stiffness of the rectangular beam and the circular beam having the same rigidity ratio $\rho = 10$ are plotted in Fig. 6, which reveals that the circular beam has higher lateral stiffness. The figure also plots

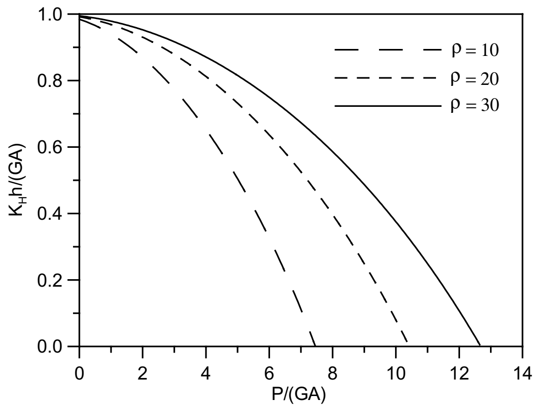

Fig. 5. Lateral stiffness of circular beams varied with compression load.

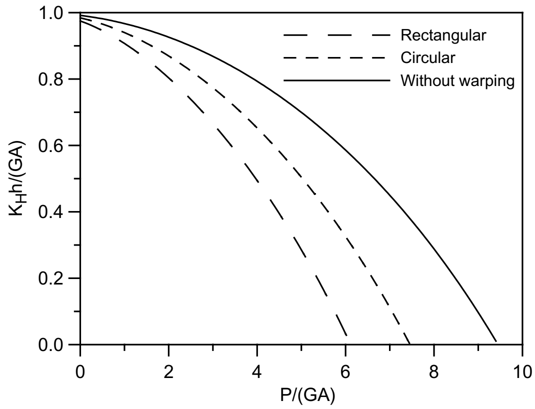

Fig. 6. Warping effect on lateral stiffness of homogeneous beams ($\rho = 10$).

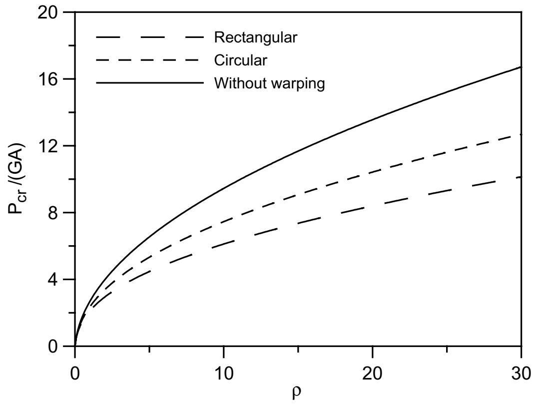

Fig. 7. Warping effect on buckling load of homogeneous beams.

the lateral stiffness without cross-section warping calculated from Eq. (77), which shows that the lateral stiffness decreases with including the effect of cross-section warping.

For the rectangular beam, the buckling load equation in Eq. (70), becomes

$$\overline{P}_{cr}^3 + \left(2 + \frac{2}{7}\pi^2\rho\right)\overline{P}_{cr}^2 + \left(1 - \frac{5}{7}\pi^2\rho\right)\overline{P}_{cr} - \left(\pi^2\rho + \frac{3}{35}\pi^4\rho^2\right) = 0 \tag{92}$$

which is a cubic equation of the buckling load P_{cr} and can be solved by the numerical method for a specified ρ value. For the circular beam, the buckling load equation is

$$\overline{P}_{cr}^3 + \left(2 + \frac{2}{9}\pi^2\rho\right)\overline{P}_{cr}^2 + \left(1 - \frac{7}{9}\pi^2\rho\right)\overline{P}_{cr} - \left(\pi^2\rho + \frac{1}{9}\pi^4\rho^2\right) = 0 \tag{93}$$

The numerically solved buckling loads of the rectangular beam and the circular beam are plotted in Fig. 7 as a function of ρ, which shows that the buckling load increases with increasing rigidity ratio. The figure also plots the buckling load without cross-section warping calculated from Eq. (81), which shows that the buckling load decreases with including the effect of cross-section warping.

6. Conclusion

A beam theory has been developed for the stability analysis of short beam in which shear deformation and warping of the cross-section are included. The warping of the cross-section is taken to be an independent kinematics quantity and corresponding force resultants has been defined. Constitutive equations relating the kinematics quantities that arise in the theory to the force quantities has been developed and equilibrium equations have been obtained by the principle of virtual work.

The flexural deformation of the beam can be described by the three quantities: lateral displacement, rotational angle of the cross-section and the multiplier of the warping shape. For the beam subjected to the external loading only at the ends of the beam, the variations of these three quantities along the beam axis are solved in closed form and expressed in terms of deformation quantities at the ends of the beam.

For the beam sustained an axial compression force and a lateral shear force at one end, the lateral stiffness of the beam, which includes the effects of stability, shear and warping, is explicitly derived. By setting the lateral stiffness equal to zero, the equation of the buckling load is established, from which the buckling load can be solved by numerical method. By setting the rigidity of cross-section warping to infinity, the warping effect is neglected and the lateral stiffness and buckling load converge to the solutions of the Haringx theory.

References

Gent, A.N., 1964. Elastic stability of rubber compression spring. Journal of Mechanical Engineering Science 6, 318–326.

Haringx, J.A., 1948. On highly compressible helical springs and rubber rods, and their application for vibration-free mountings—Part III. Philips Research Reports 4, 206–220.

Kelly, J.M., 1994. The influence of plate flexibility on the buckling load of elastomeric isolators. Report UCB/EERC-94/03, Earthquake Engineering Research Center, University of California, Berkeley.

Kelly, J.M., 1997. Earthquake-Resistant Design with Rubber, second ed. Springer-Verlag, London.

Tsai, H.-C., Hsueh, S.-J., 2001. Mechanical properties of isolation bearings identified by a viscoelastic model. International Journal of Solid and Structures 38, 53–74.